

Figure 7.25 A typical CMOS process flow illustrating the difference between FEOL and BEOL processes.

FRONT END of the Line (FEOL)

- * shallow trench Isolation (STI)
- * Twin - tubs (twin wells)
- * single level poly silicon
- * Low-doped drain extensions

Backend of the line (BEOL)

- * fully planarized dielectrics
- * planarized tungsten contacts and VIA plugs
- * Aluminum metallization

In the following we want describe

- * wafer cleaning
- * individual photolithographic steps
- * Back side film removal after CVD
- * metrology to measure thickness, critical dimensions, etc.

Table 7.1 Masks used in our generic CMOS process.

Layer name	Mask	Aligns to level	Times used	Purpose
1 (active)	Clear	aligns to notch	1	Defines active areas
2 (p-well)	Clear	1	2	Defines NMOS sidewall implants and p-well
3 (n-well)	Dark	1	2	Defines PMOS sidewall implants and n-well
4 (poly1)	Clear	1	1	Defines polysilicon
5 (n-select)	Dark	1	2	Defines nLDD and n+
6 (p-select)	Dark	1	2	Defines pLDD and P+
7 (contact)	Dark	4	1	Defines contact to poly and actives areas
8 (metal1)	Clear	7	1	Defines metal1
9 (via1)	Dark	8	1	Defines via1 (connects M1 to M2)
10 (metal2)	Clear	9	1	Defines metal2
passivation	Dark	Top-level metal	1	Defines bond pad opening in passivation

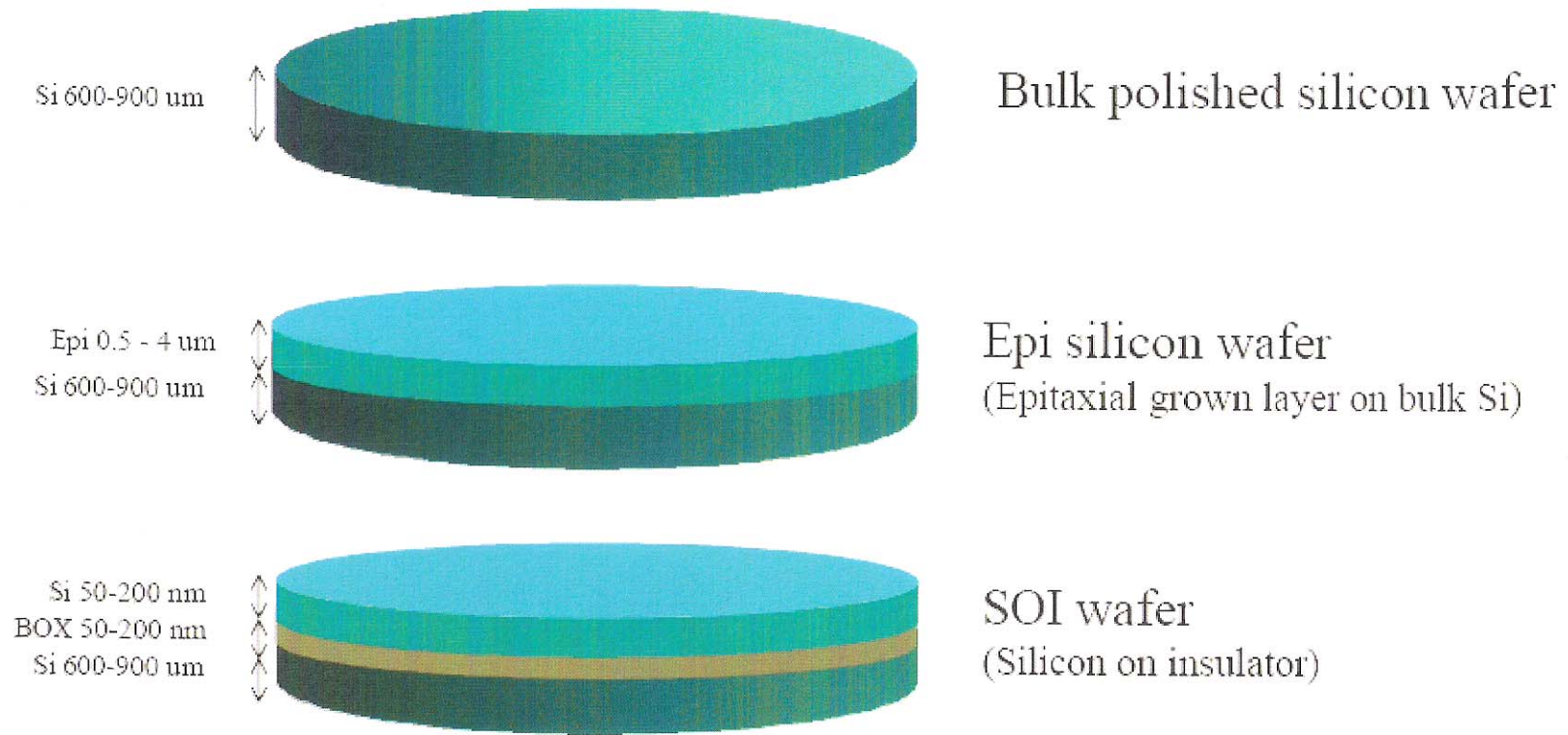


Figure 7.26 The three general types of silicon wafers used for CMOS fabrication.

4)

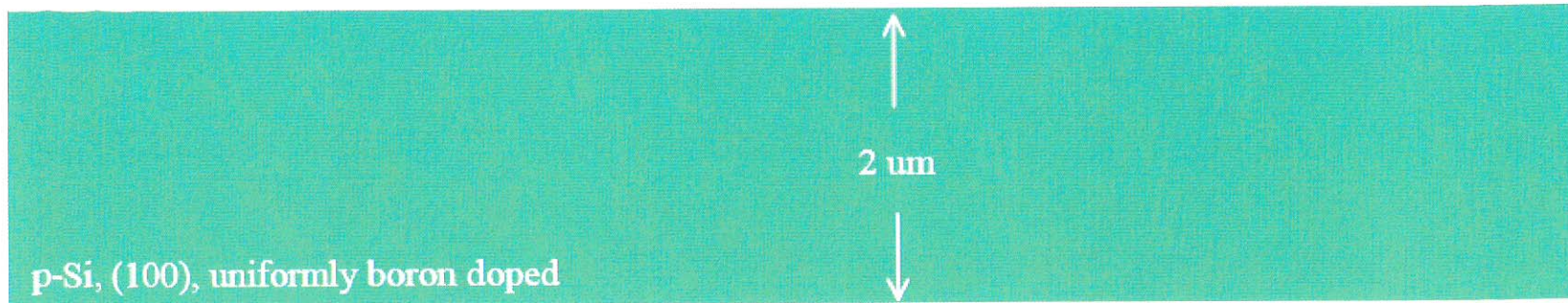


Figure 7.27 Simulated cross-sectional view (the top 2 μm) of the bulk wafer in Fig. 7.26.



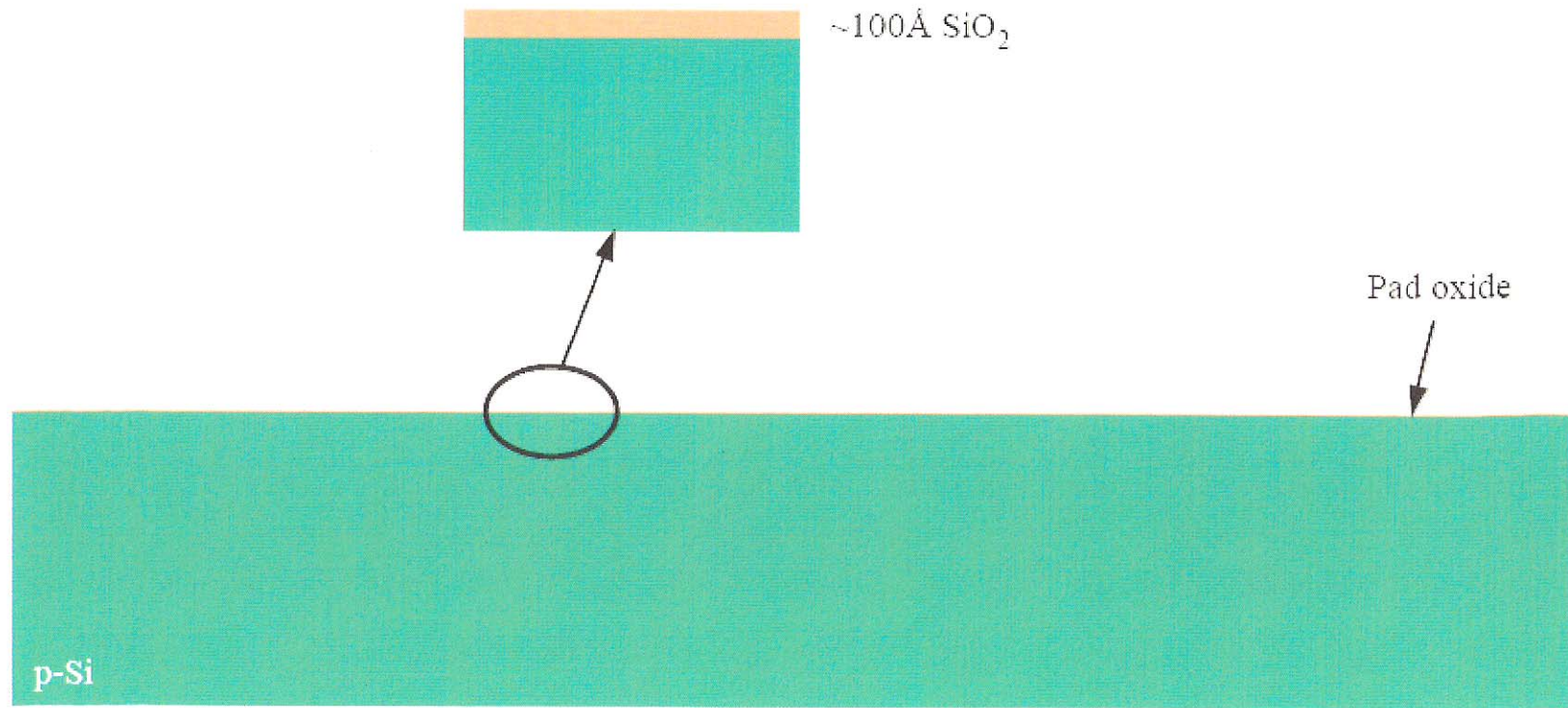
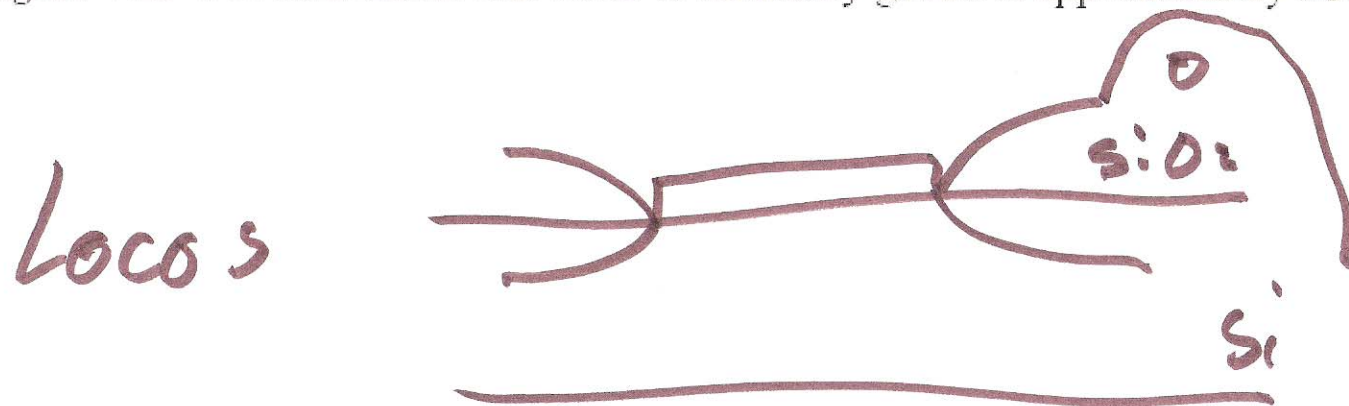


Figure 7.28 STI film stack. The oxide is thermally grown at approximately $900\text{ }^\circ\text{C}$ with dry



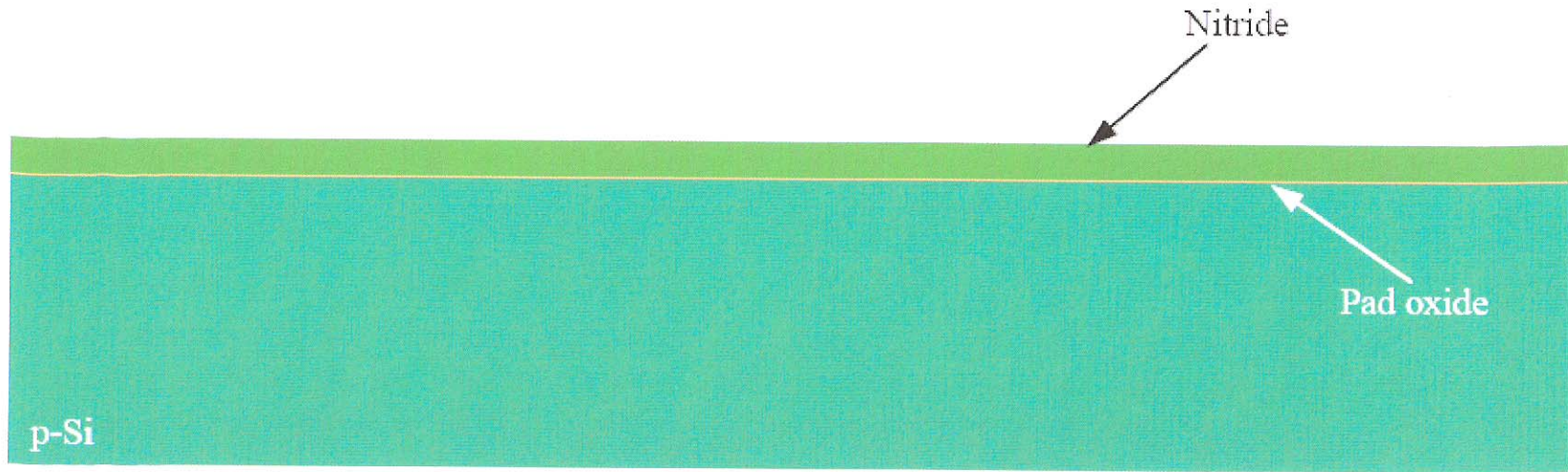
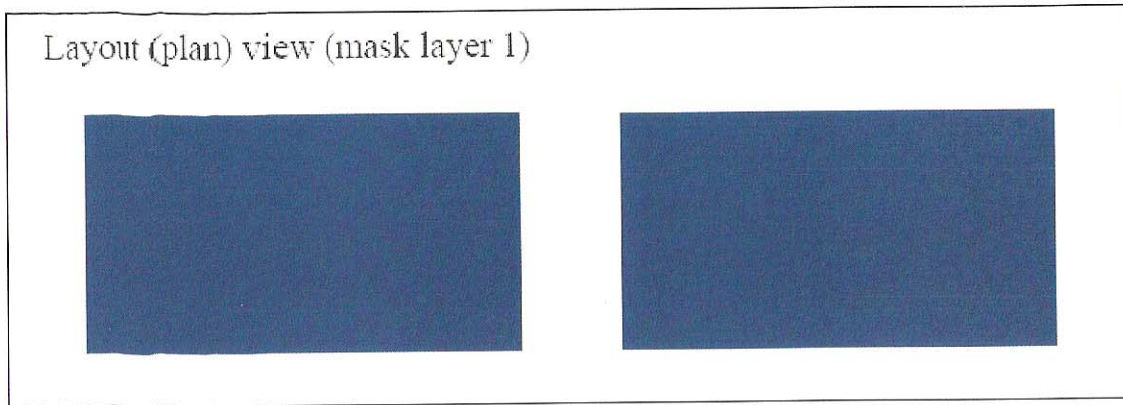


Figure 7.29 STI film stack. Silicon nitride deposited by LPCVD at approximately 800 °C.





Cross-section

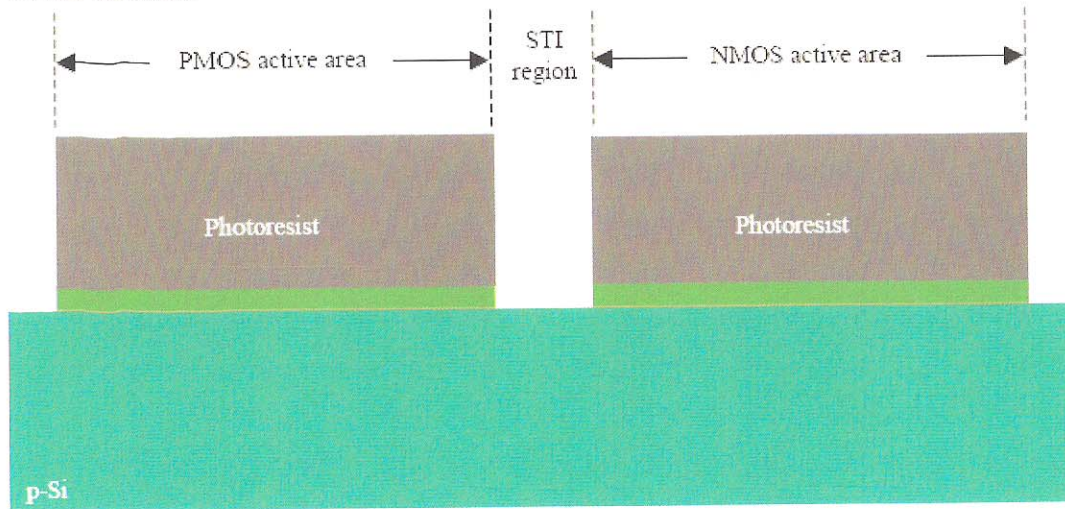


Figure 7.30 STI definition, photolithography and nitride/pad oxide etch with fluorocarbon-based RIE.

8)

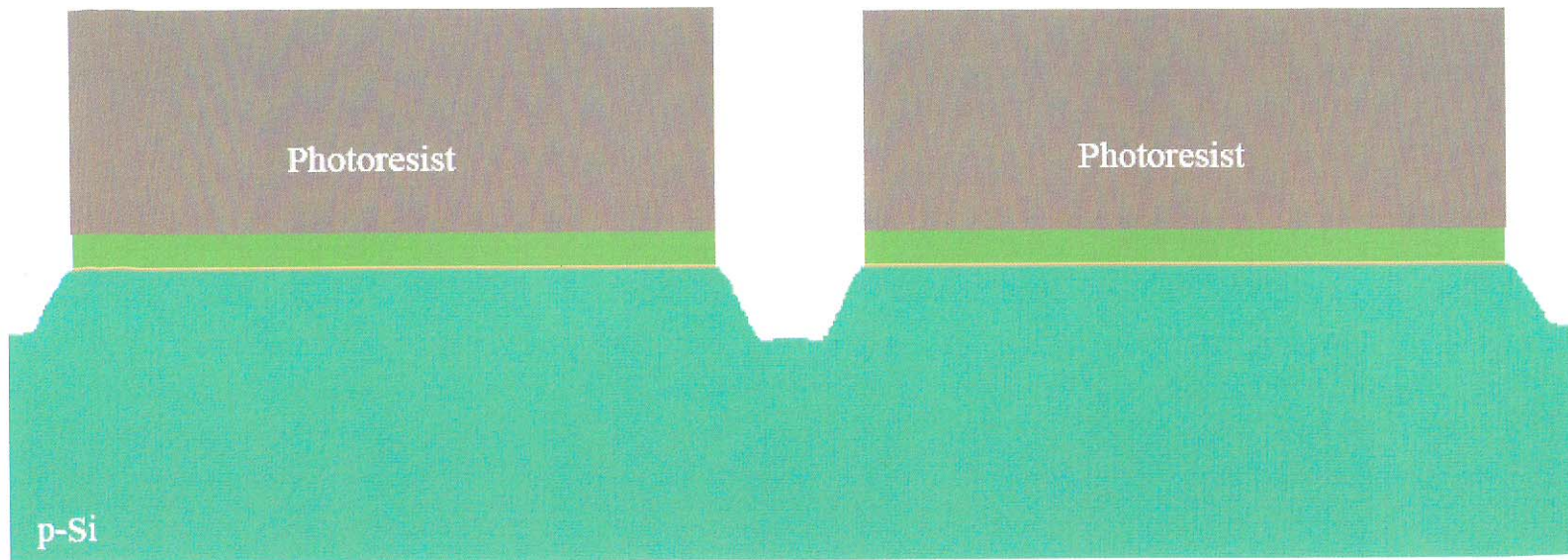


Figure 7.31 Timed silicon trench reactive ion etch.

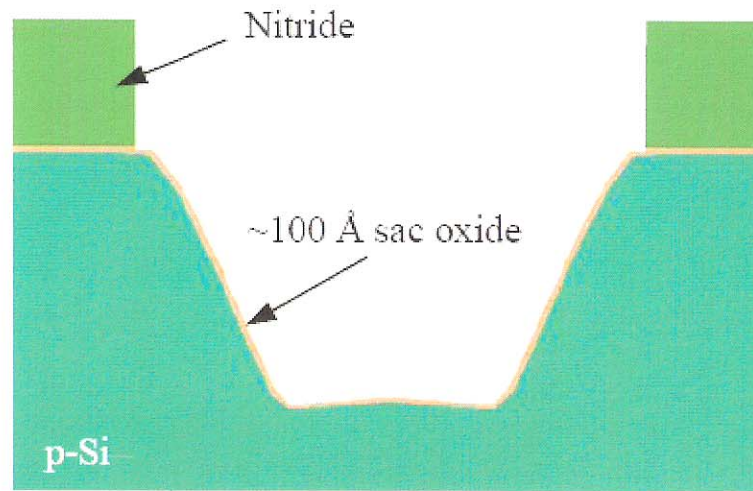
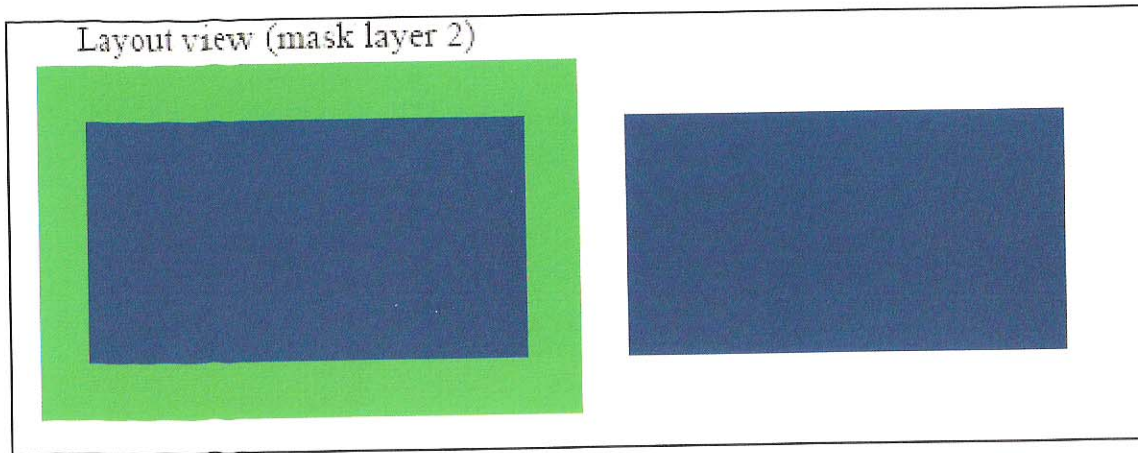


Figure 7.32 Cross section showing post STI resist strip followed by the dry thermal oxidation (at 900 °C) of a sacrificial (sac) oxide in the trench.



Cross-section

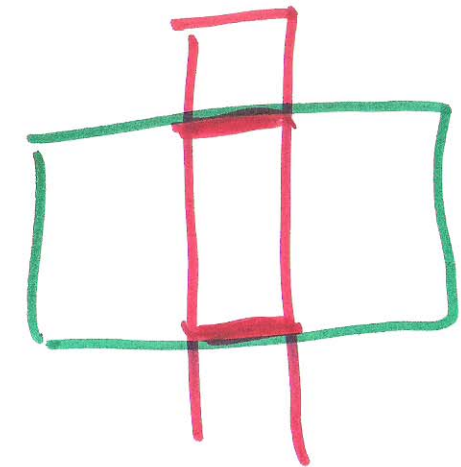
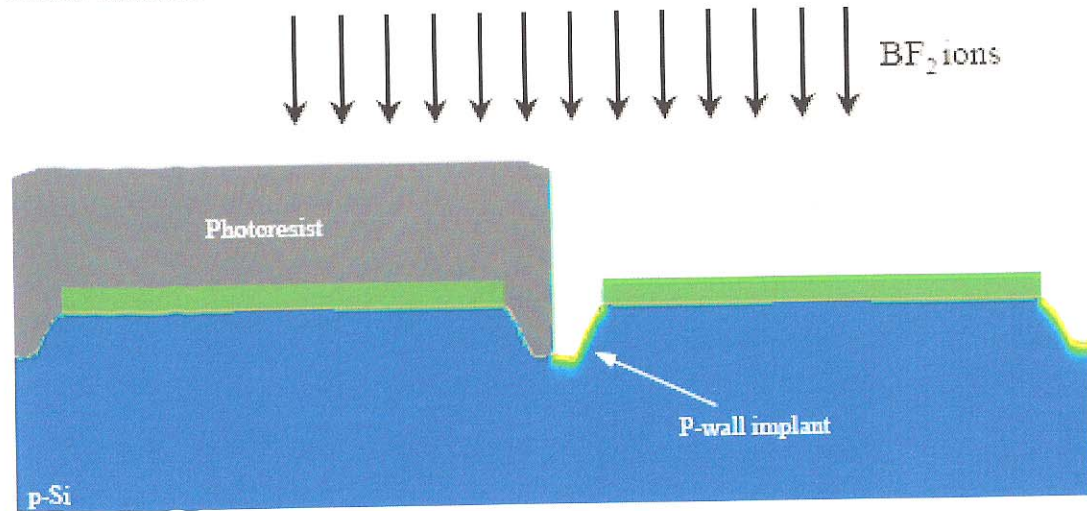


Figure 7.33 P-wall sidewall formation via photolithography and BF_2 implantation.

11)

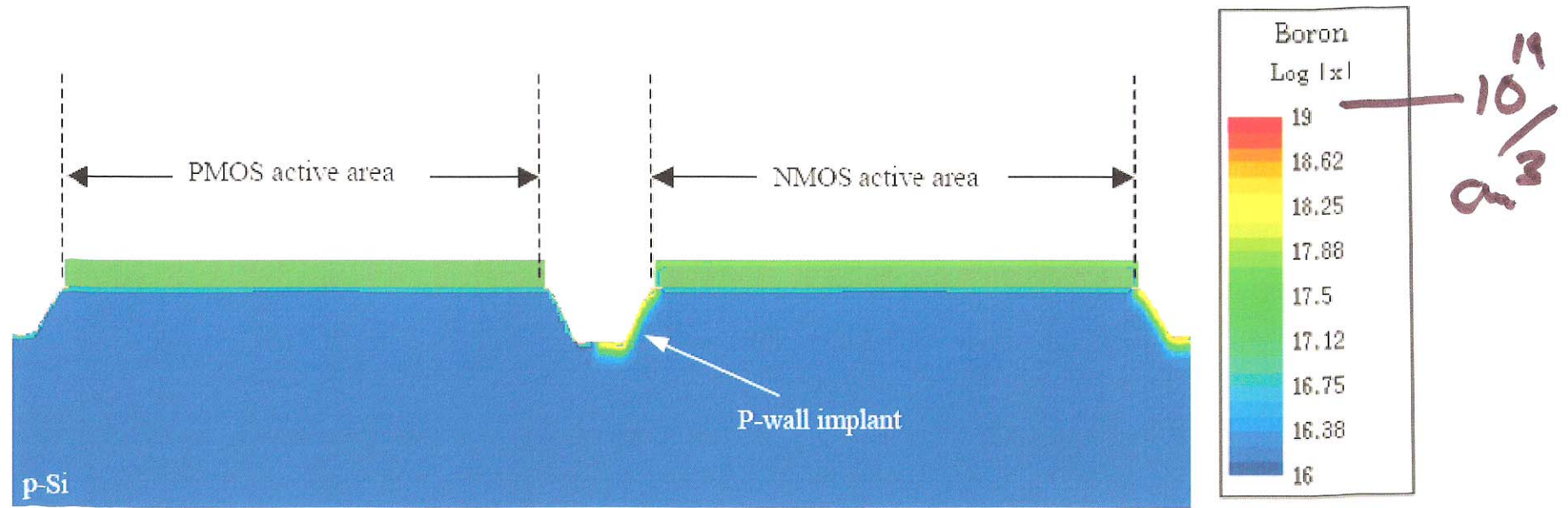
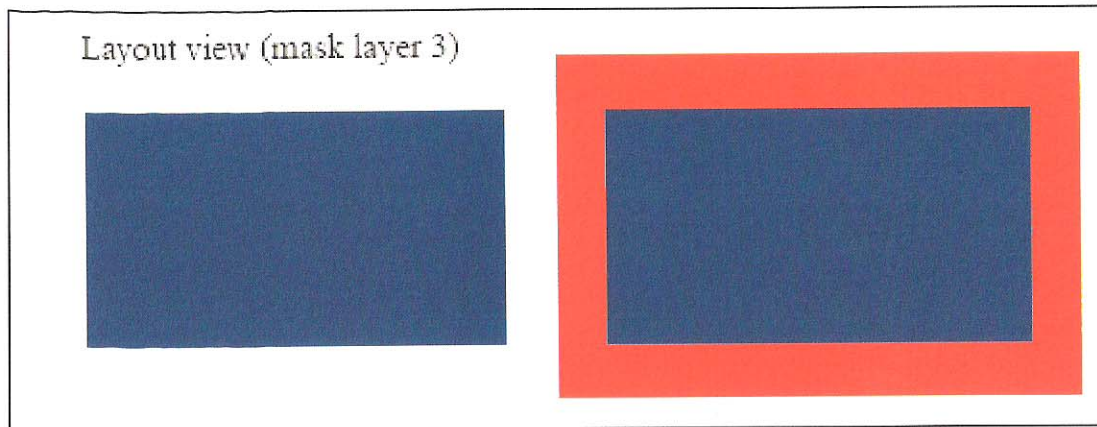


Figure 7.34 Post p-wall photoresist strip using O_2 plasma and wet processing.

12)



Cross-section

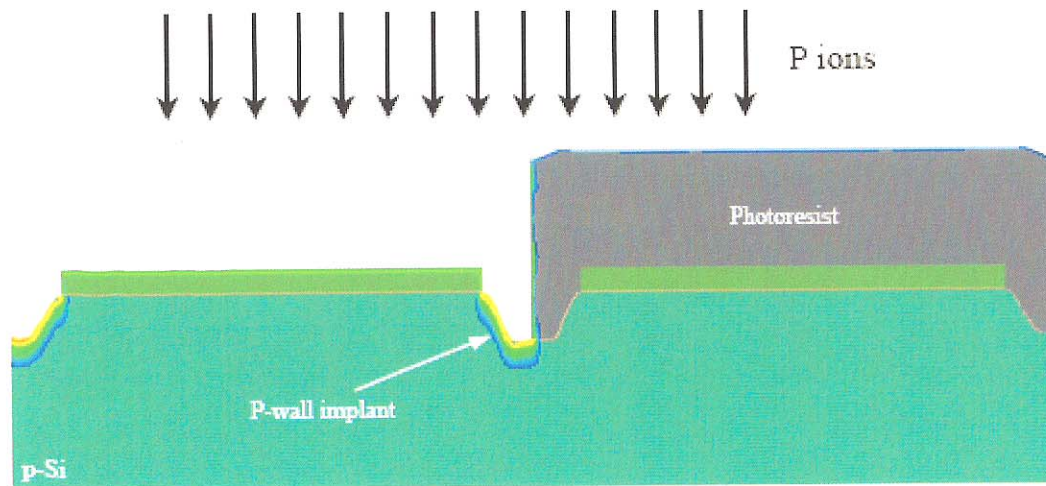


Figure 7.35 N-wall sidewall formation via photolithography and P implantation.

(13)

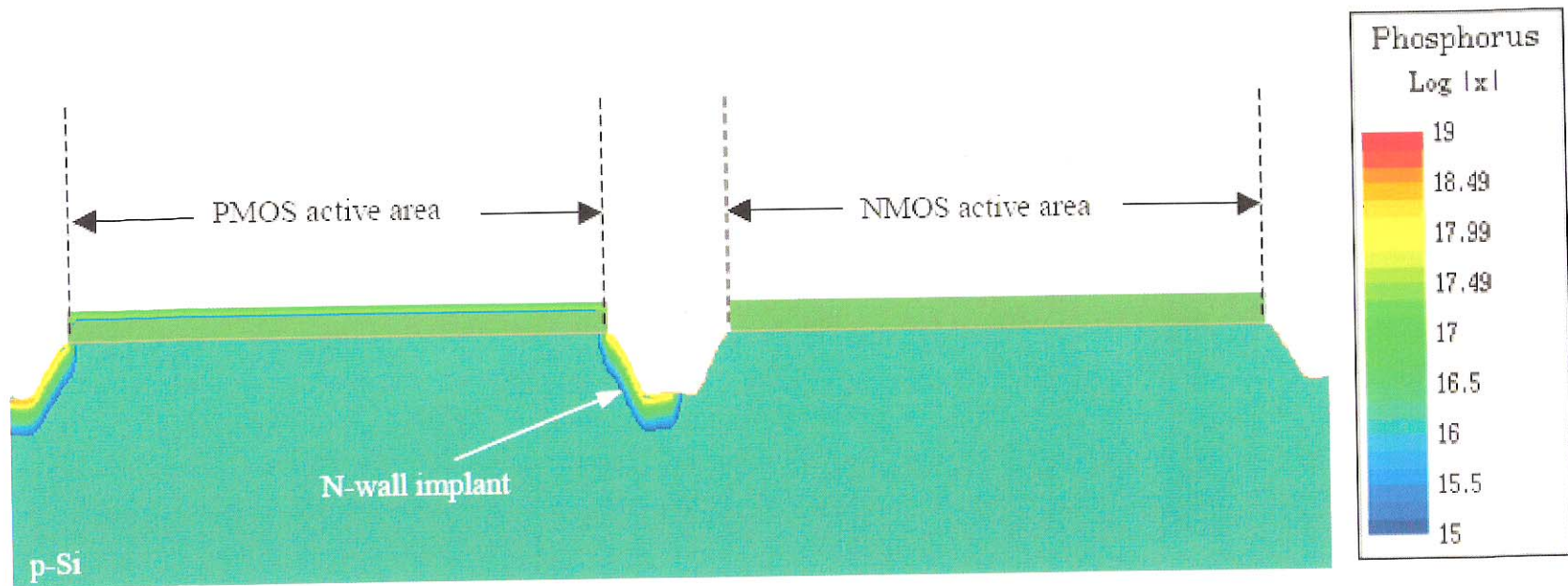


Figure 7.36 Post n-wall photoresist strip using O_2 plasma and wet processing.

14)

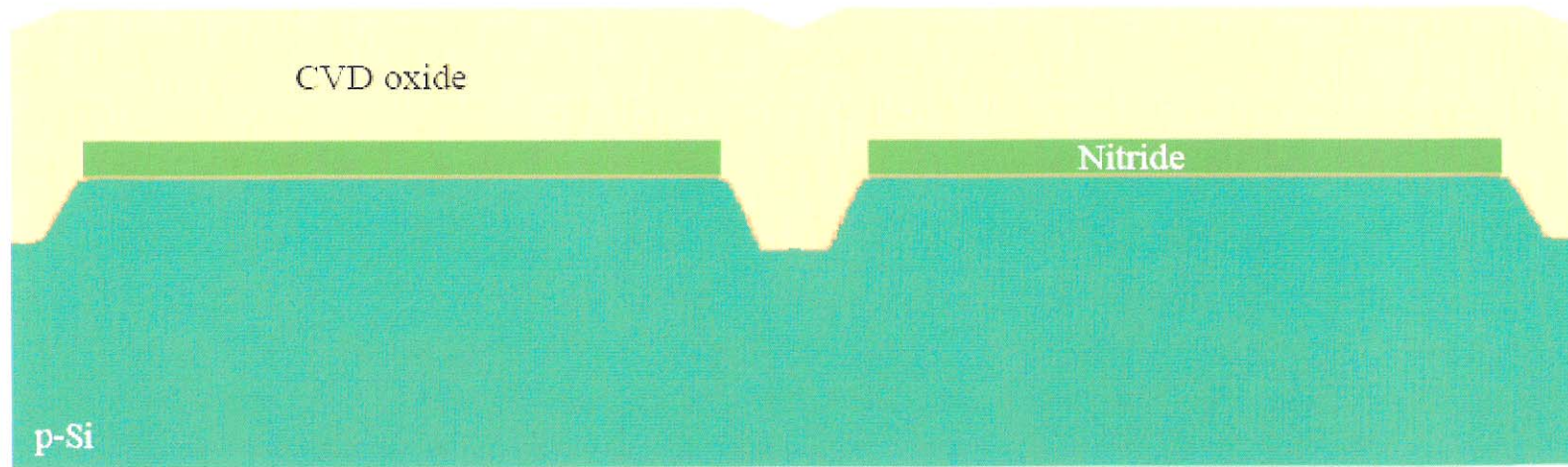


Figure 7.37 High-quality, 100 Å thick liner oxide, is thermally grown at 900 °C. High-density plasma (HDP) CVD trench fill at room temperature. Notice the trenches are overfilled.

15)

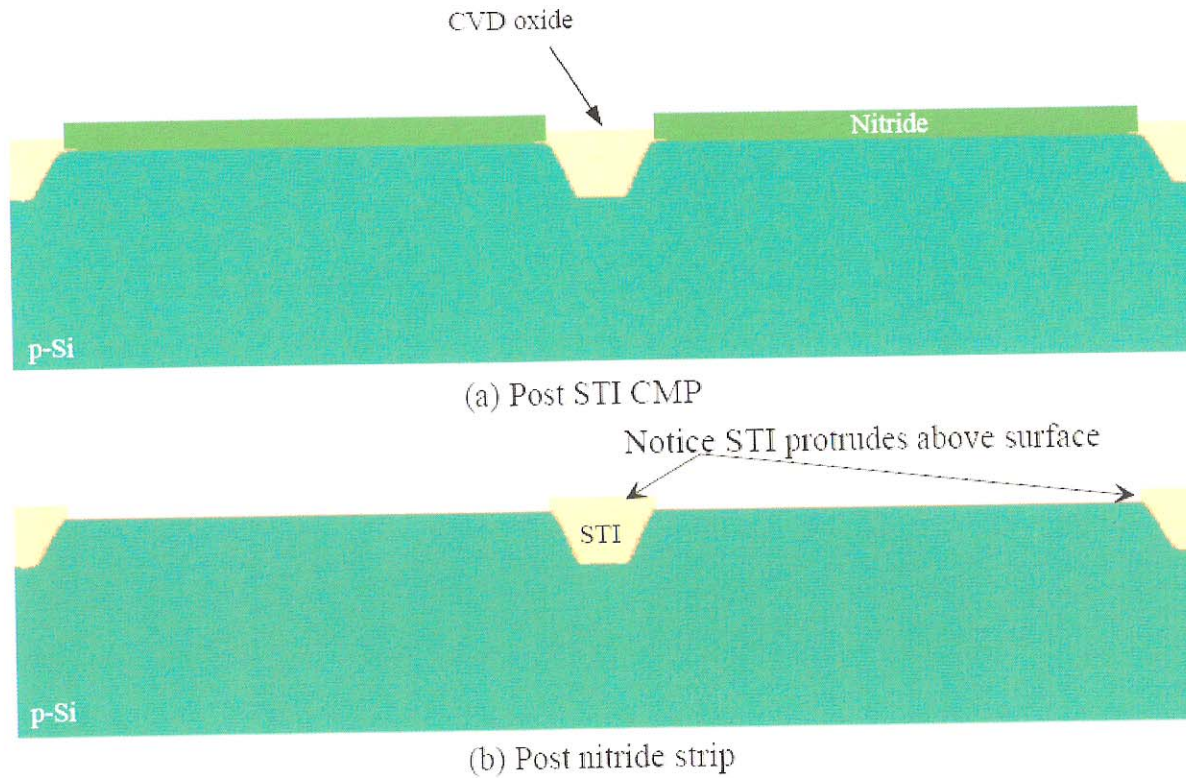
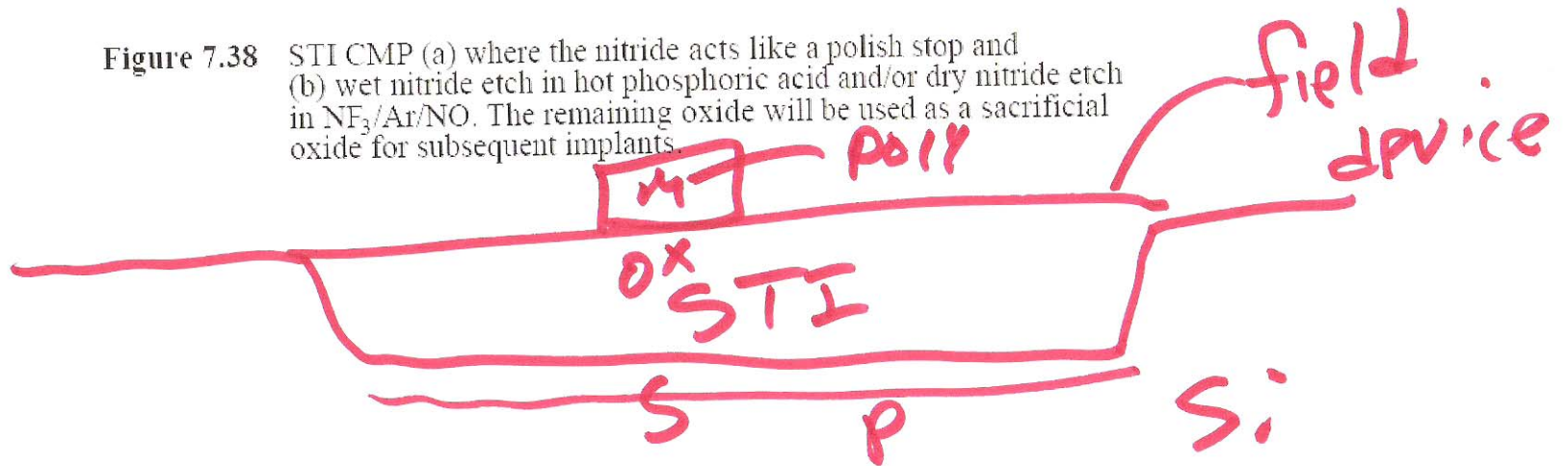


Figure 7.38 STI CMP (a) where the nitride acts like a polish stop and (b) wet nitride etch in hot phosphoric acid and/or dry nitride etch in $\text{NF}_3/\text{Ar}/\text{NO}$. The remaining oxide will be used as a sacrificial oxide for subsequent implants.



16)

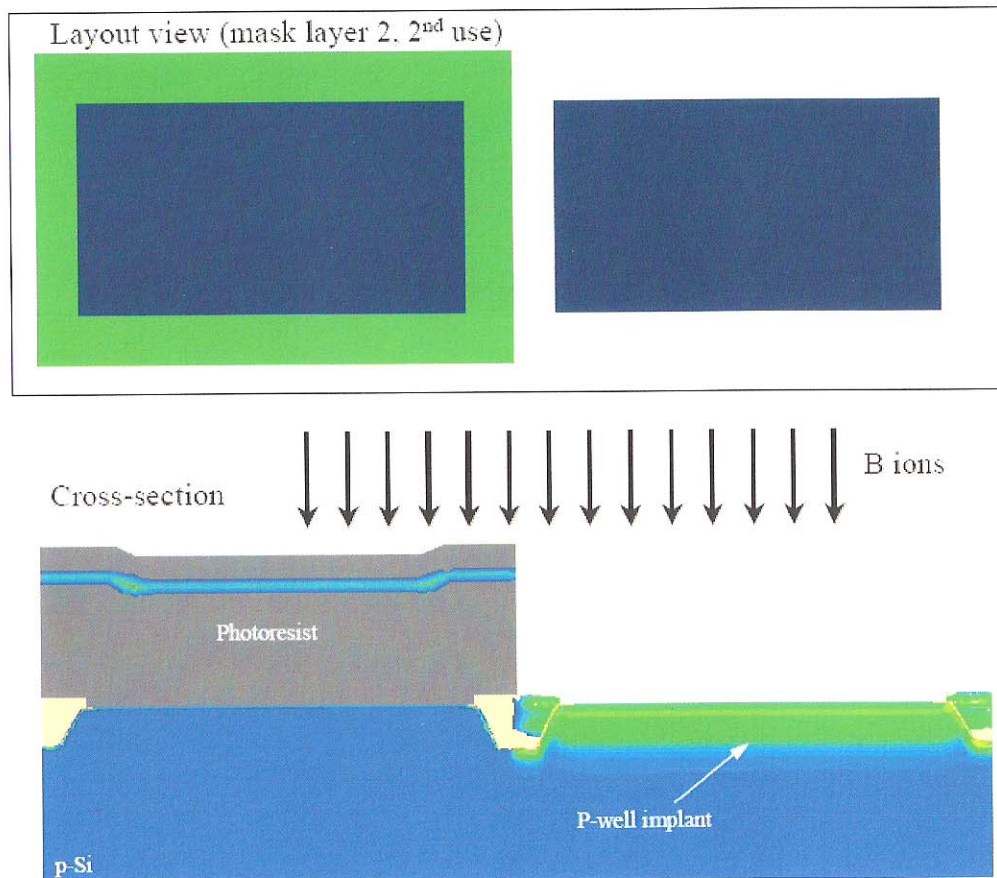


Figure 7.39 P-well formation via photolithography and *B* implantation.

17)

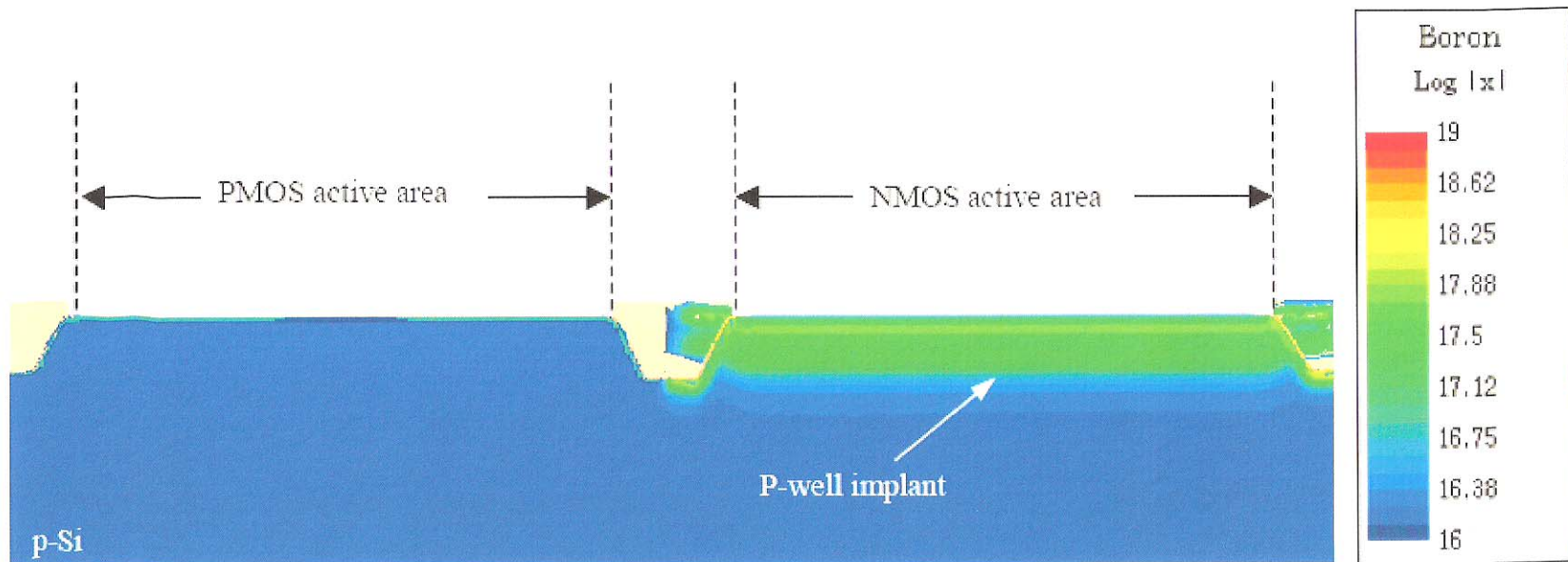
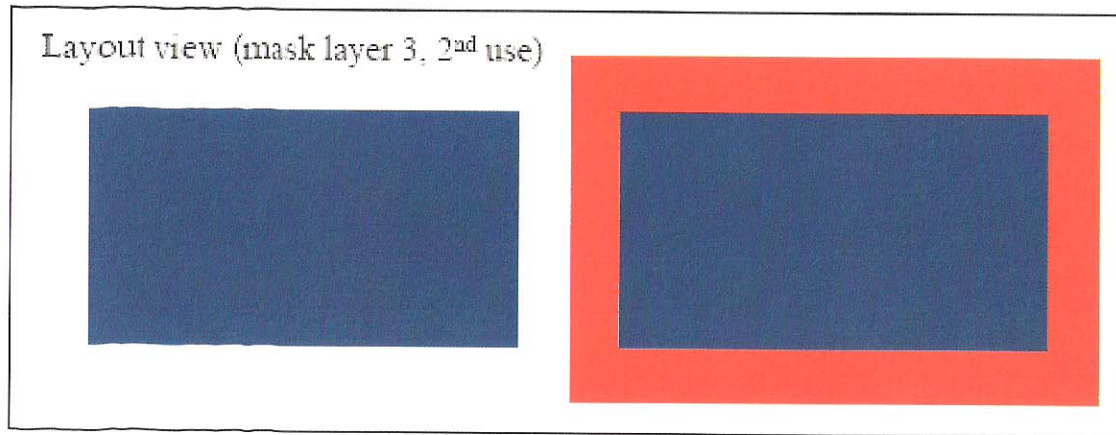


Figure 7.40 Post p-well photoresist strip using O_2 plasma and wet processing.

18)



Cross-section

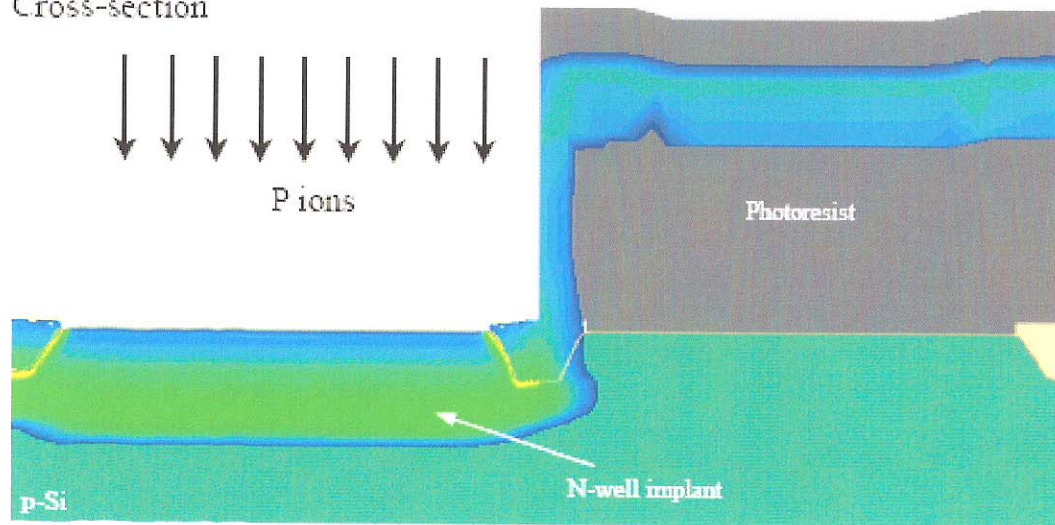


Figure 7.41 N-well formation via photolithography and P implantation.

19)

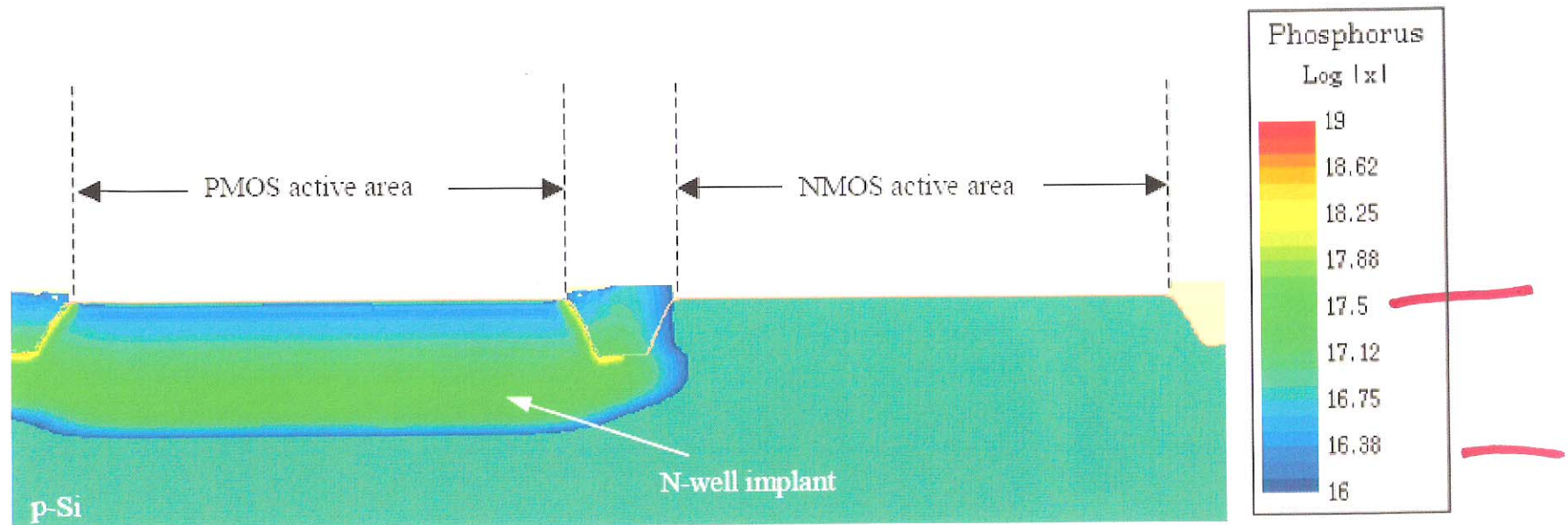


Figure 7.42 Post n-well photoresist strip using O_2 plasma and wet processing.

retrograde profile

w)

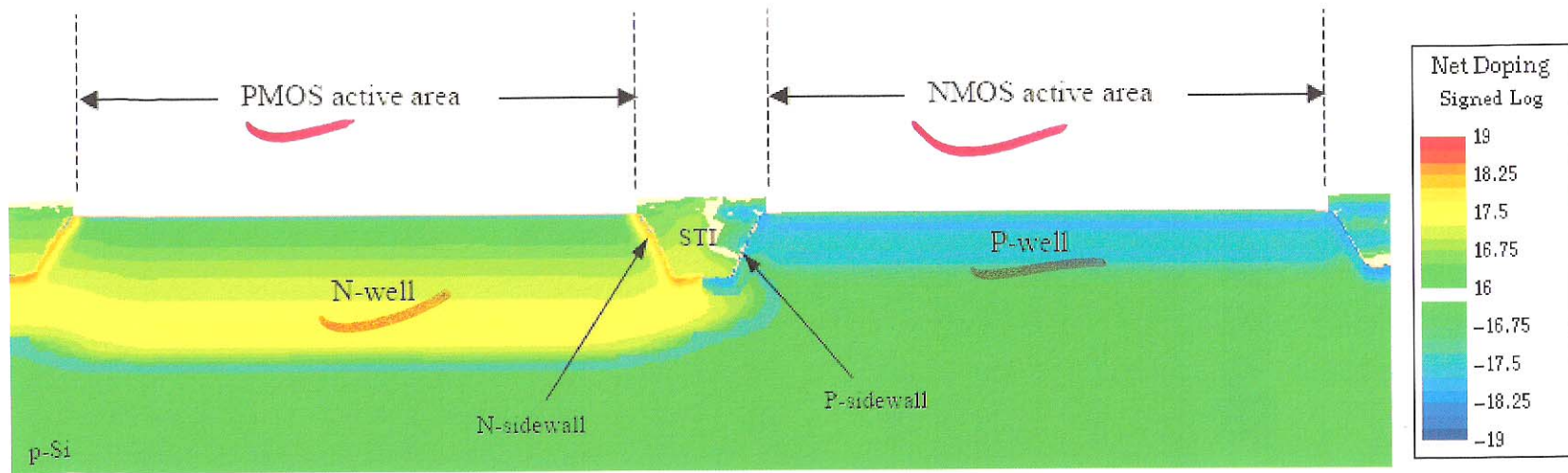
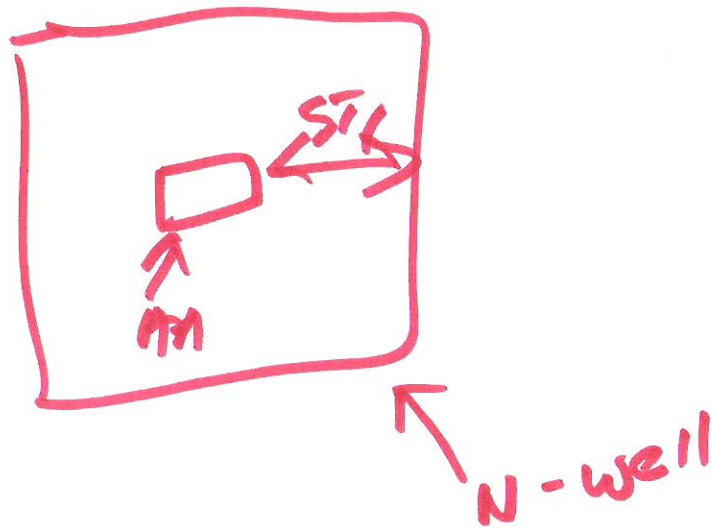


Figure 7.43 Net doping profile of both the n-well and the p-well.



21)

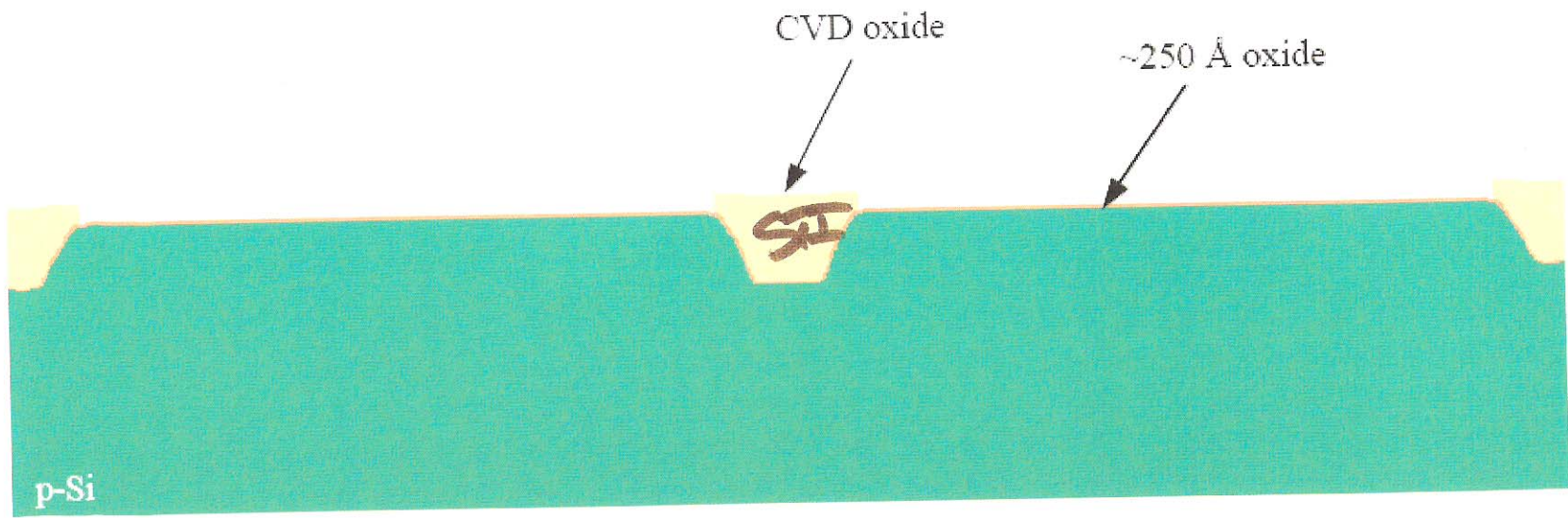


Figure 7.44 Wet etch the remaining trench stack oxide using buffered *HF*. Sacrificial oxide formation using dry thermal oxidation at approximately 900 °C.

N-well
p-well
not shown

22)

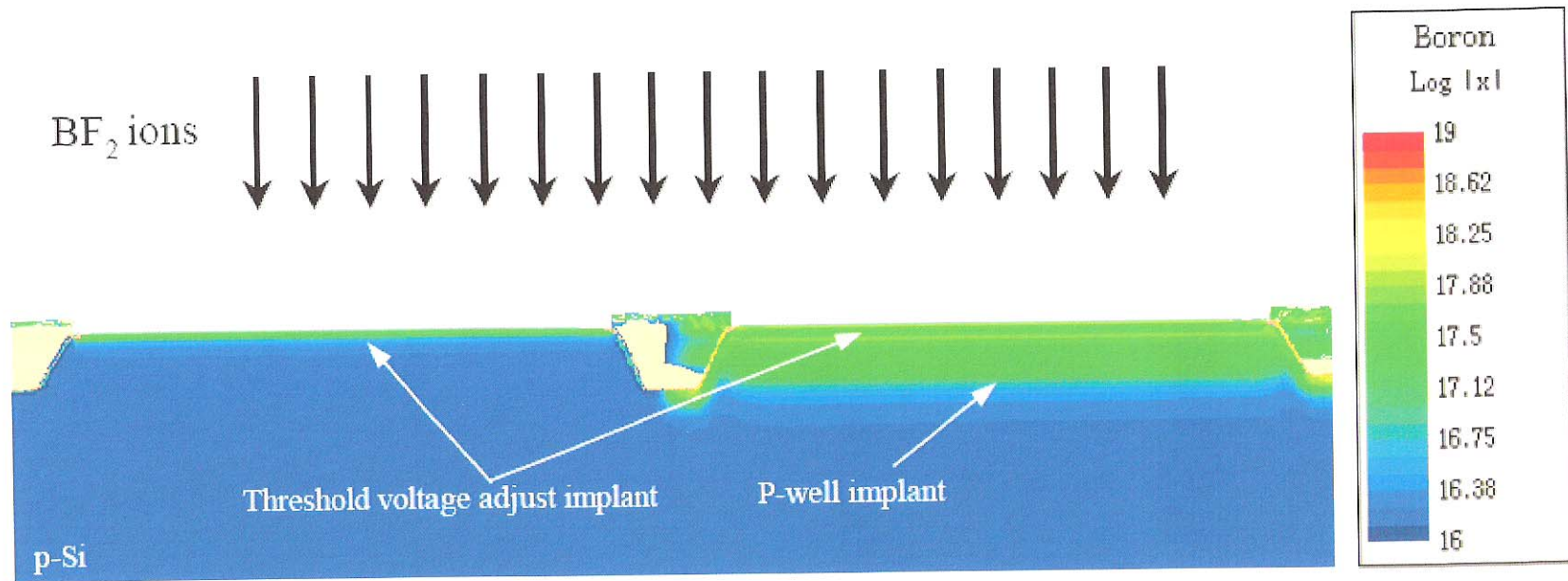


Figure 7.45 Blanket low-energy BF_2 implant for NMOS and PMOS threshold voltage adjust.

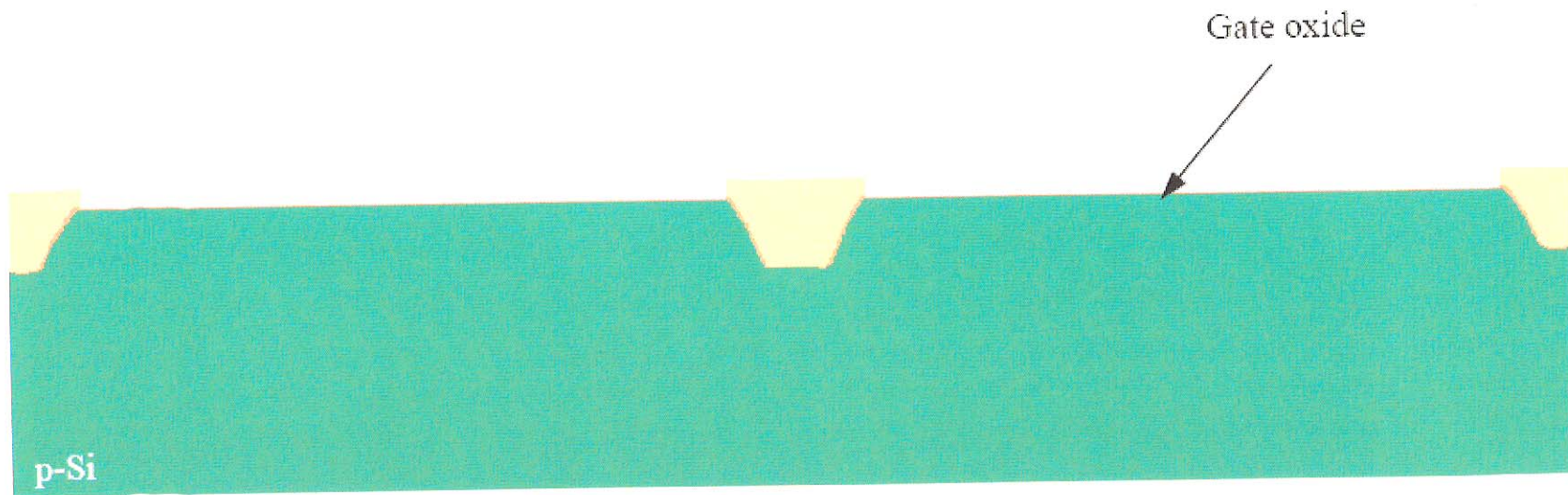


Figure 7.46 Removal of sacrificial oxide using buffered *HF* followed by gate dielectric formation using dry oxidation in an ambient of O_2 , NO and/or N_2O .

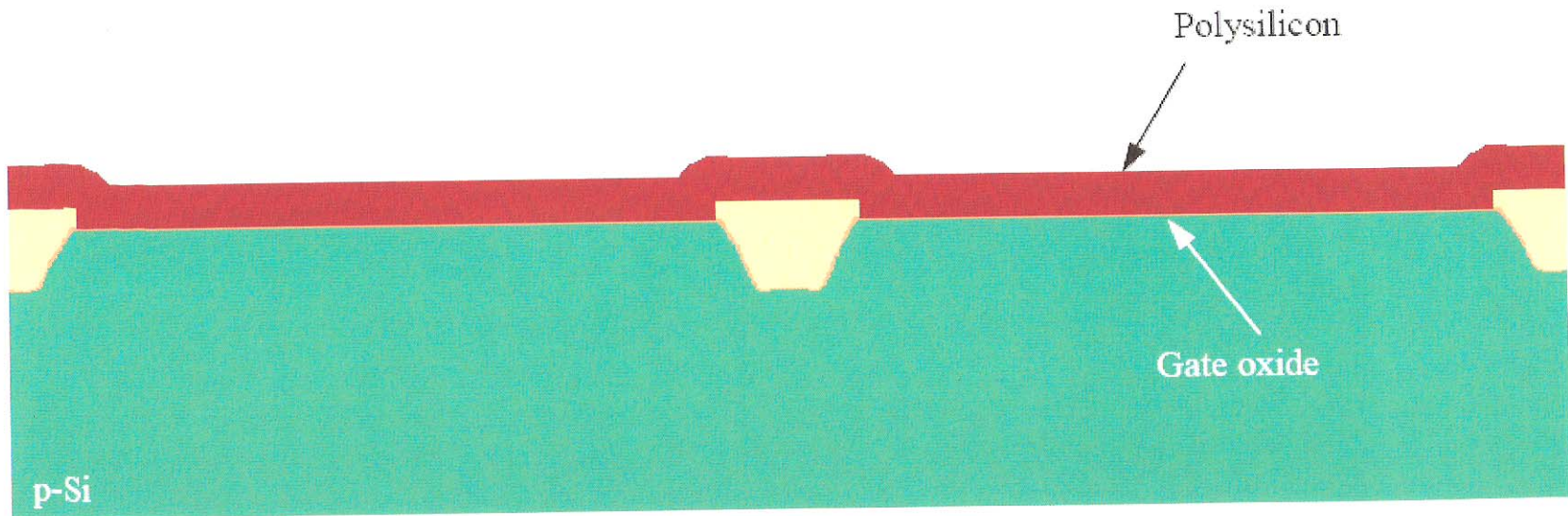


Figure 7.47 Polysilicon deposition via LPCVD at approximately 550 °C. Note the polysilicon deposition must occur immediately following gate oxidation.

25)

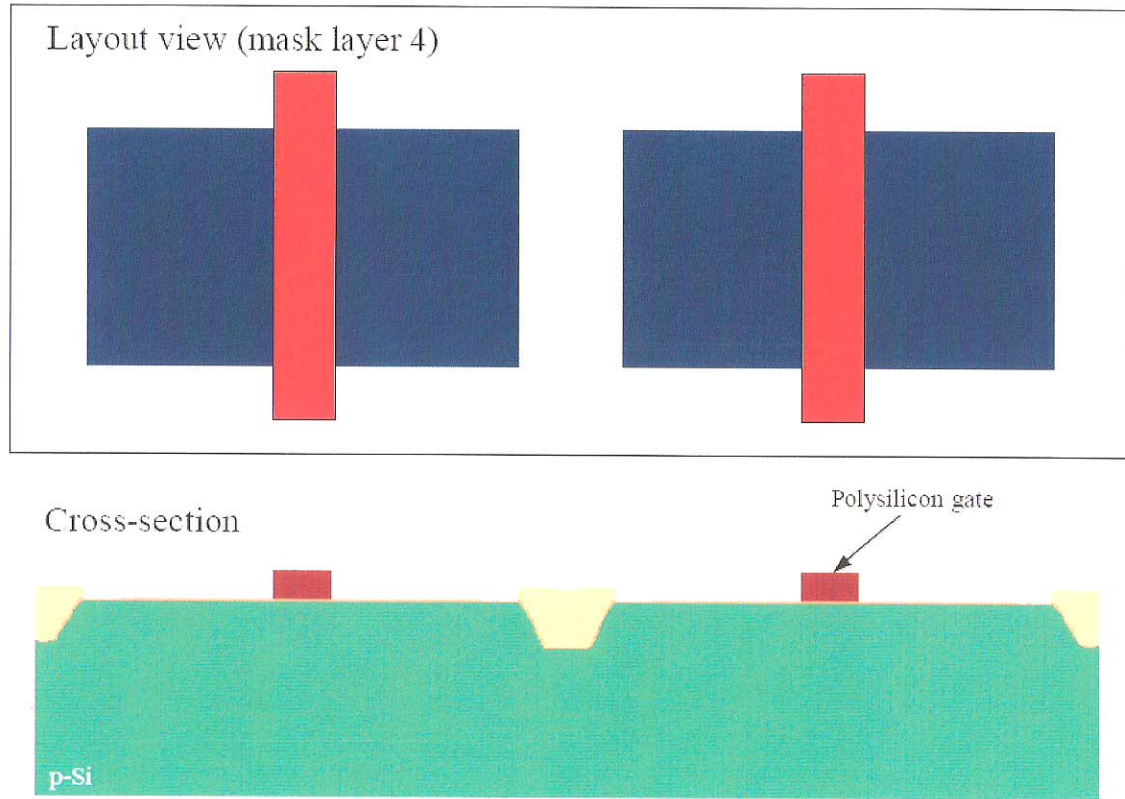


Figure 7.48 Gate electrode and local interconnect photolithography and polysilicon reactive ion etching.

26)

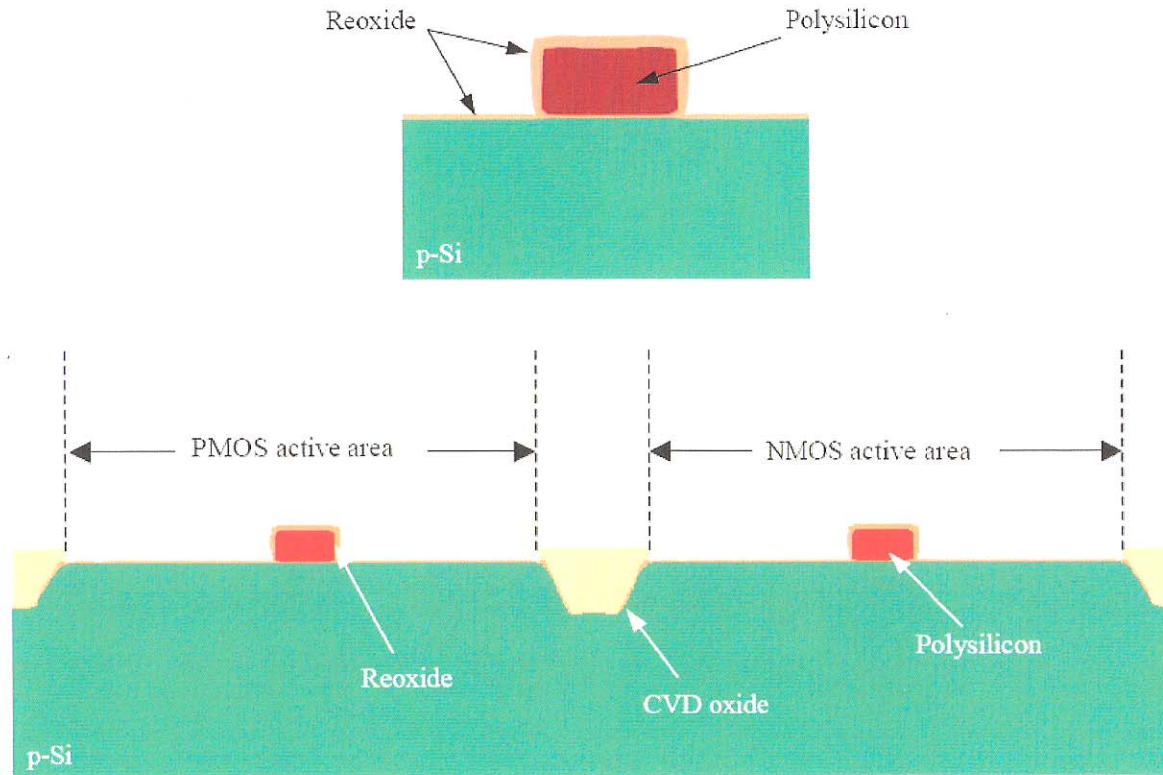
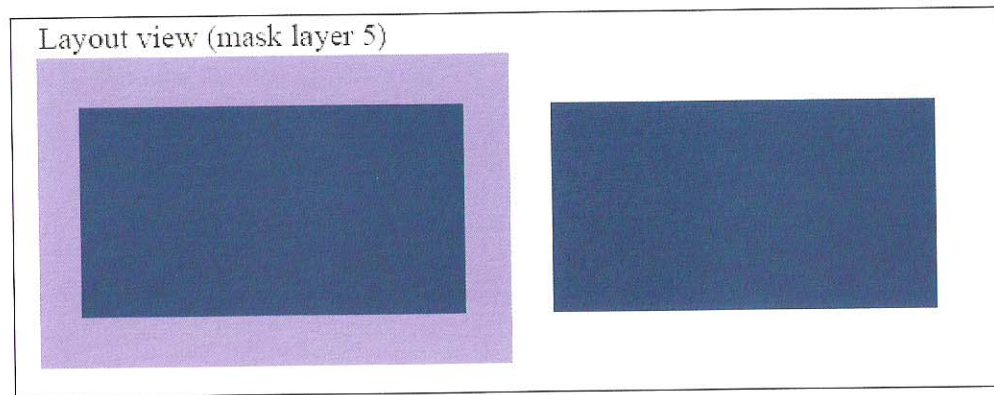


Figure 7.49 Polysilicon reoxidation using dry O_2 at approximately 900°C . Notice the resulting oxide is thicker on the polysilicon than on the active silicon.

21)



Cross-section

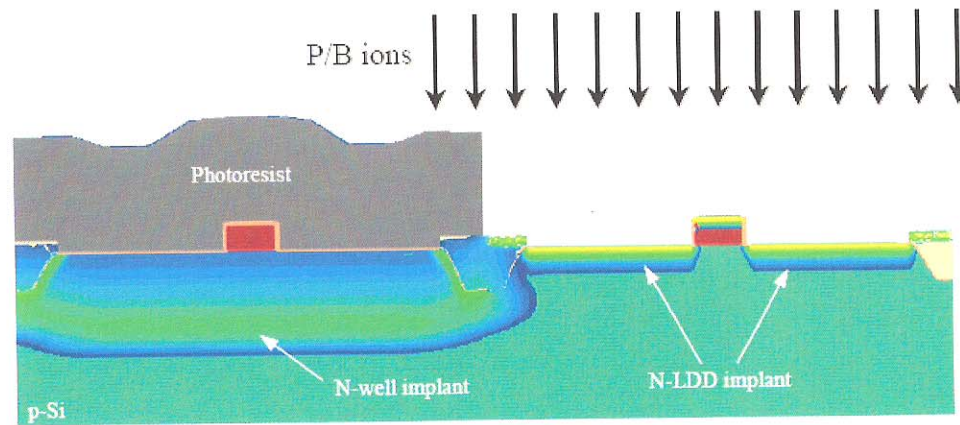
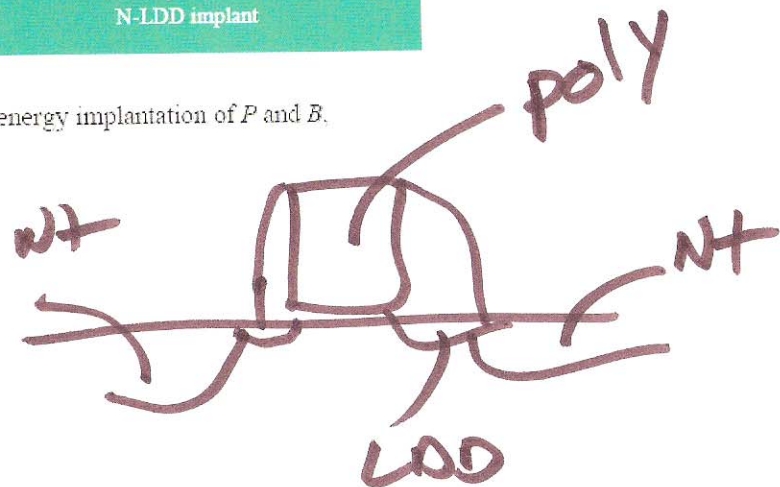


Figure 7.50 N-LDD/n-pocket formation using low energy implantation of *P* and *B*.



20)

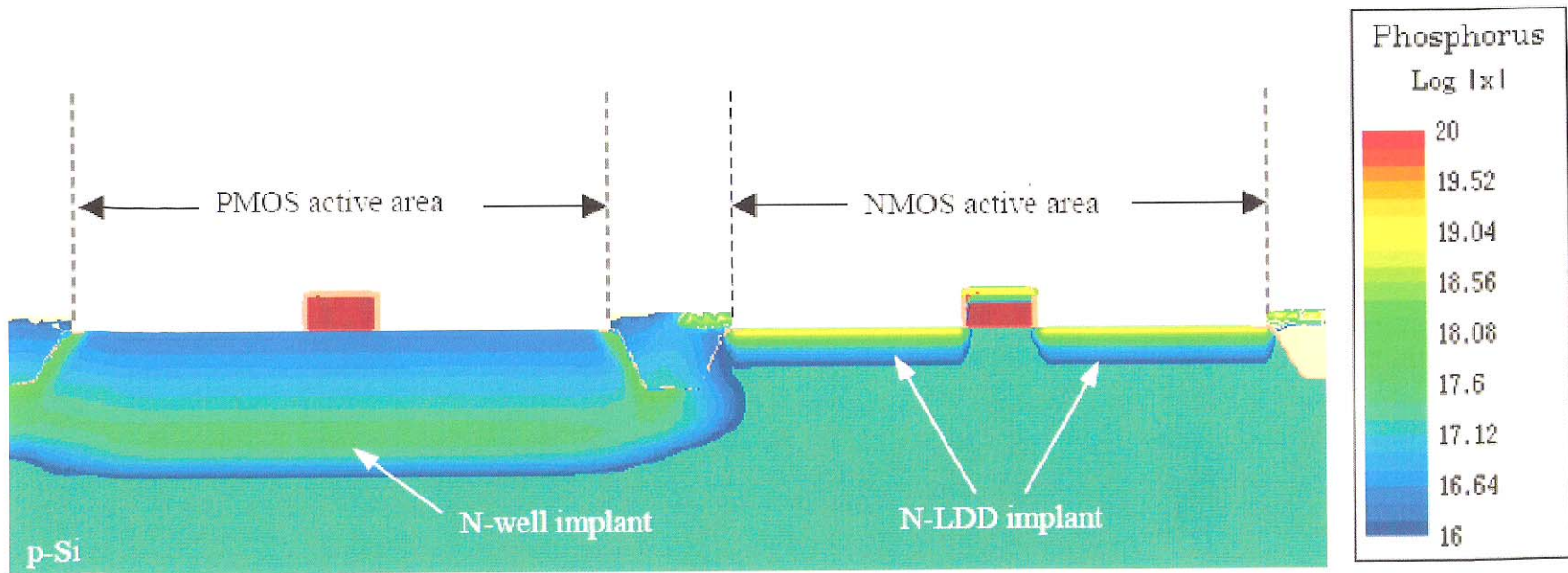


Figure 7.51 Post N-LDD resist strip using O_2 plasma and wet processing.

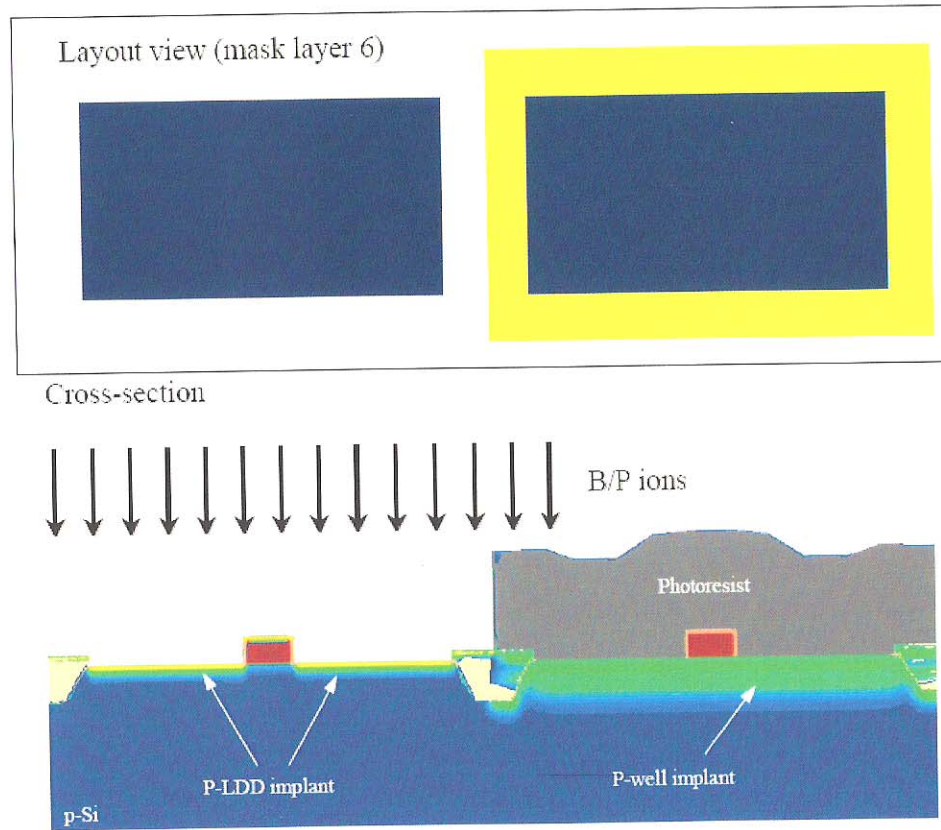


Figure 7.52 P-LDD/p-pocket formation using low energy implantation of *B* and *P*, respectively.

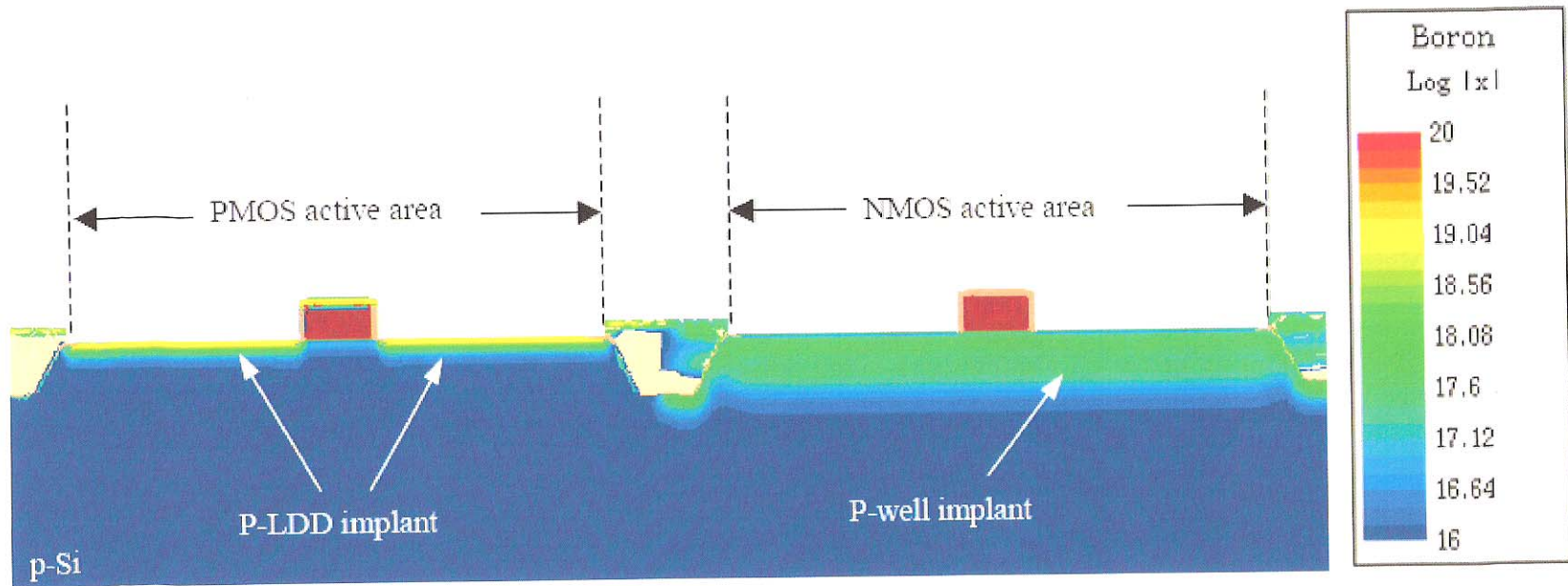


Figure 7.53 Post P-LDD resist strip using O_2 plasma and wet processing.

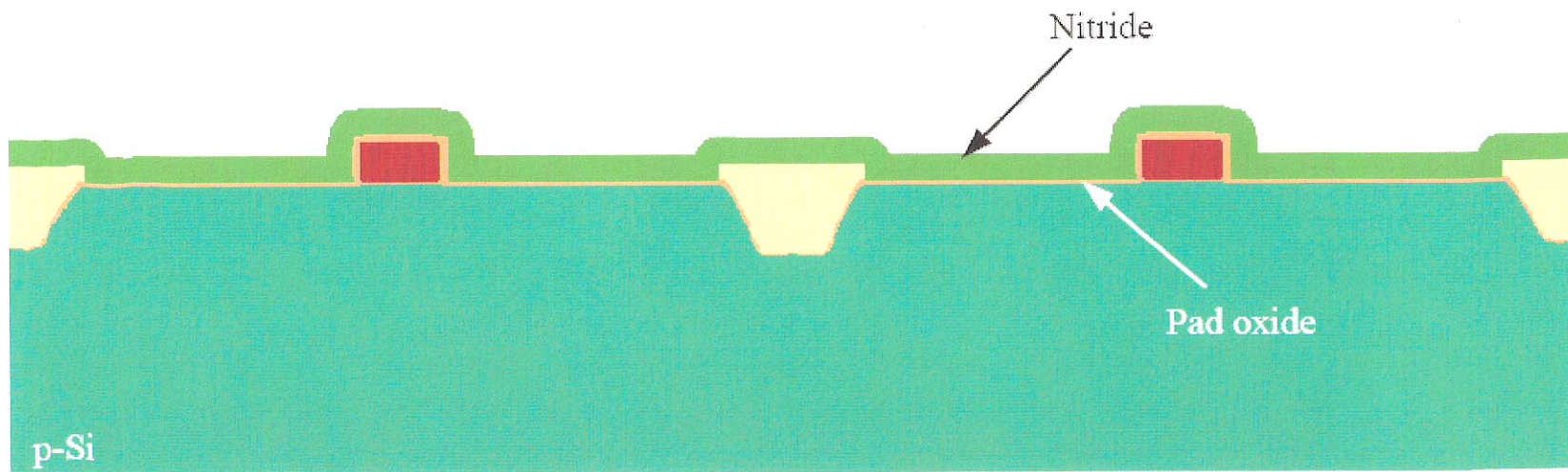


Figure 7.54 Sidewall spacer nitride deposition using LPCVD at approximately 800 °C.

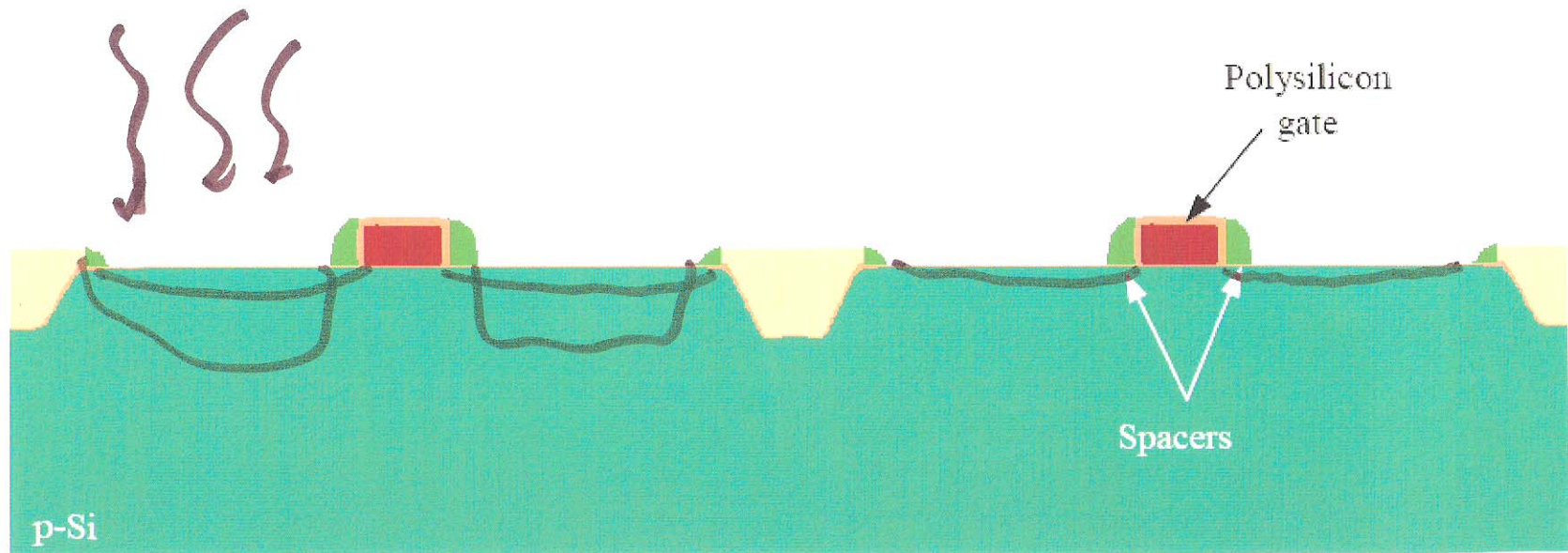
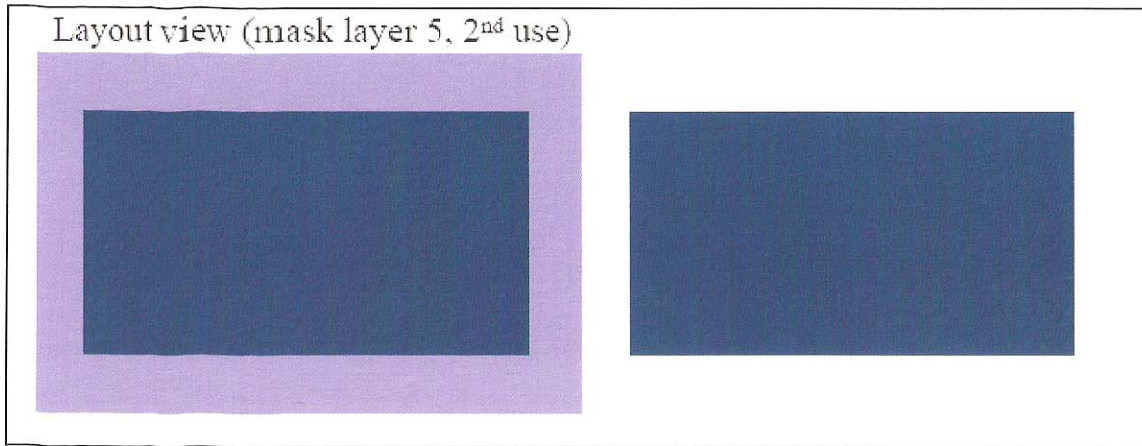


Figure 7.55 Dry, anisotropic, end-pointed reactive ion etch of spacer nitrate yielding gate sidewall spacers.



Cross-section

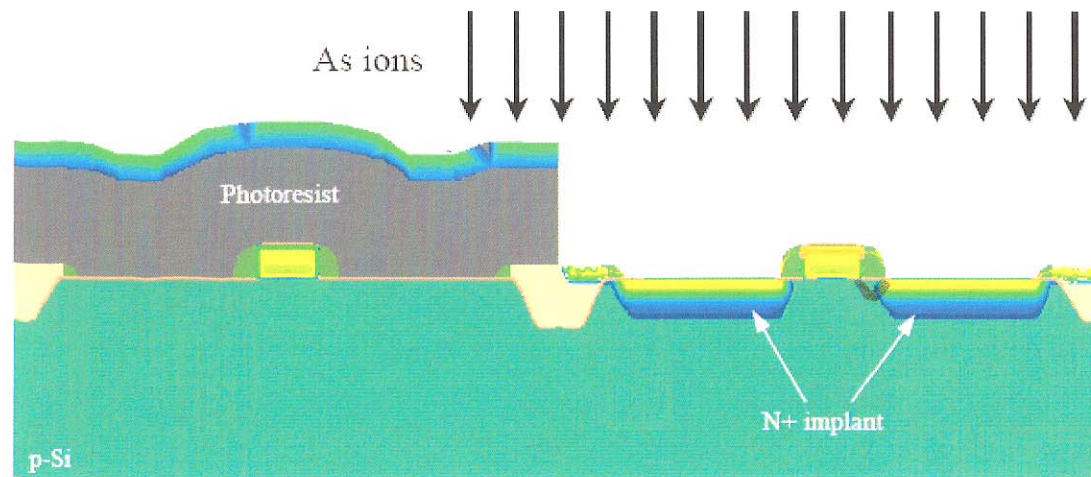


Figure 7.56 N⁺ source/drain formation using a low energy, high dose implantation of As.

34)

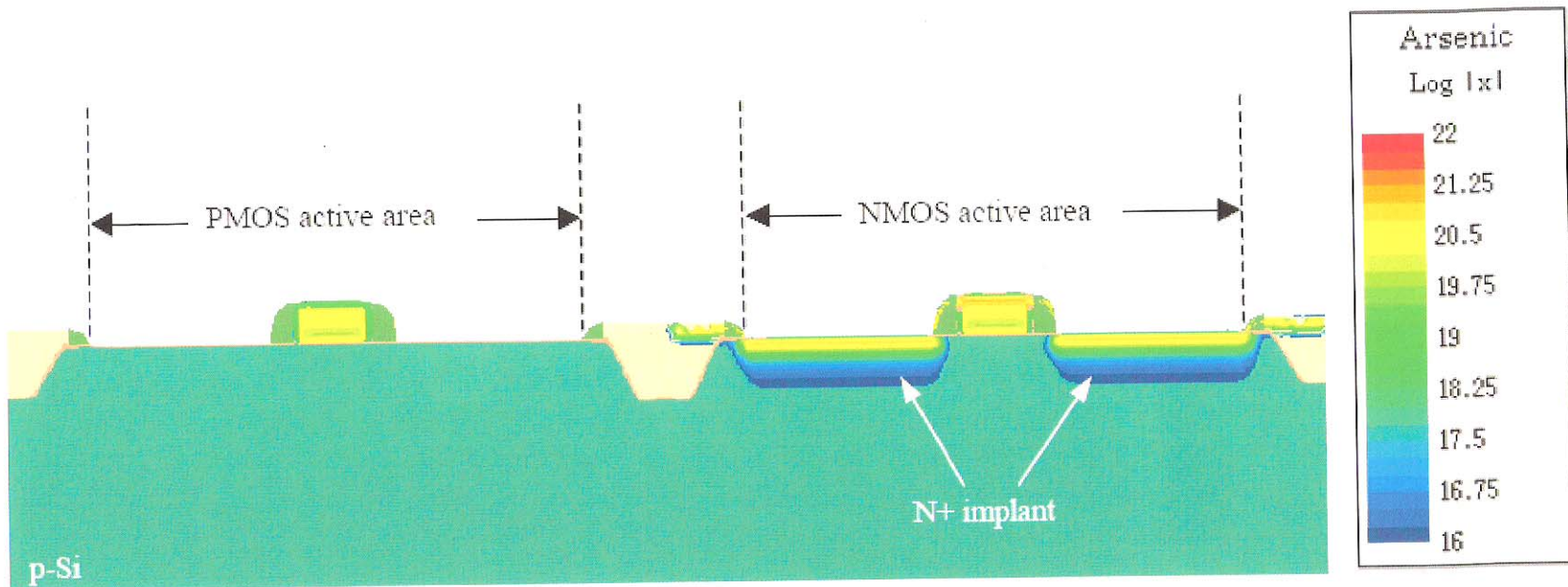
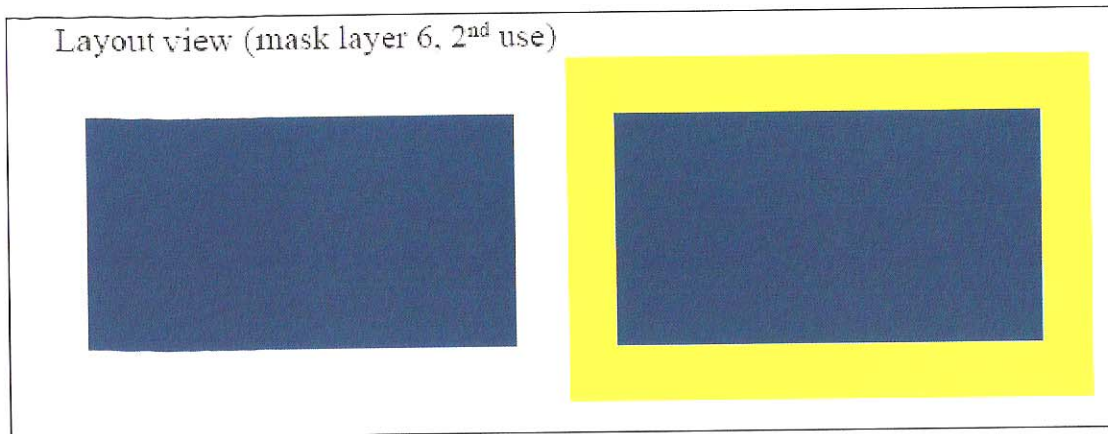


Figure 7.57 Post n+ resist strip using O_2 plasma and wet processing.



Cross-section

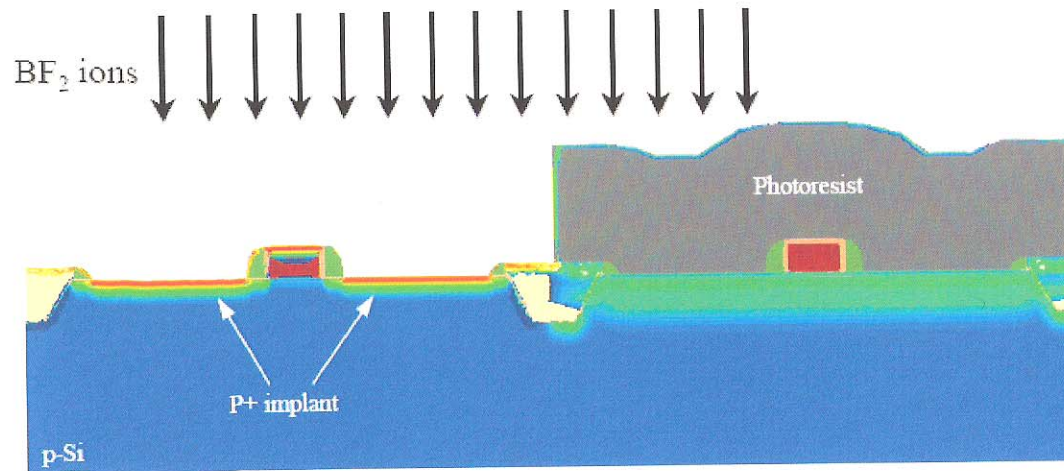


Figure 7.58 P+ source/drain formation using a low energy, high dose implantation of BF_2 .

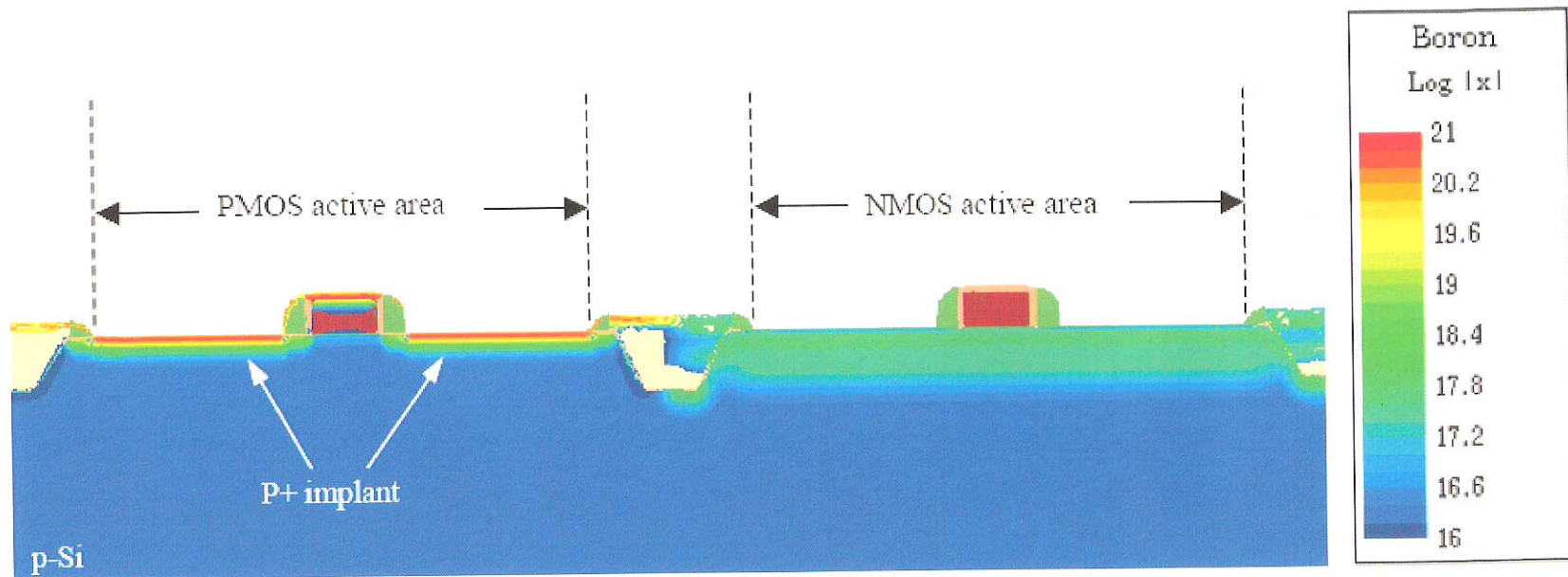


Figure 7.59 Post p+ resist strip using O_2 plasma and wet processing.

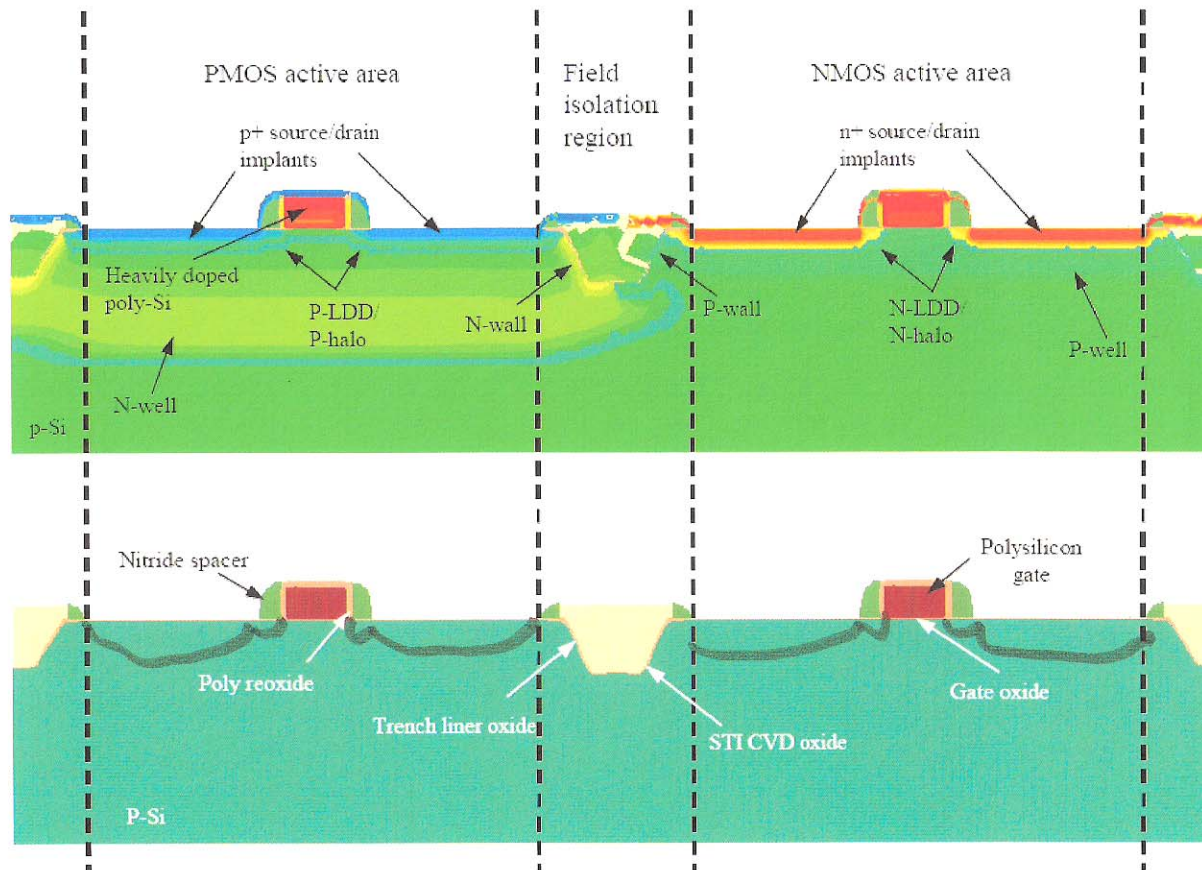


Figure 7.60 Summary of the FEOL features.

35:36

38)